

Communication

Sensitivity-enhanced IPAP-SOFAST-HMQC for fast-pulsing 2D NMR with reduced radiofrequency load

Thomas Kern, Paul Schanda, Bernhard Brutscher *

Laboratoire de RMN, Institut de Biologie Structurale Jean-Pierre Ebel, CEA, CNRS, UJF, 41 rue Jules Horowitz, 38027 Grenoble Cedex, France

Received 12 October 2007; revised 21 November 2007

Available online 19 December 2007

Abstract

The SOFAST-HMQC experiment [P. Schanda, B. Brutscher, Very fast two-dimensional NMR spectroscopy for real-time investigation of dynamic events in proteins on the time scale of seconds, *J. Am. Chem. Soc.* 127 (2005) 8014–8015] allows recording two-dimensional correlation spectra of macromolecules such as proteins in only a few seconds acquisition time. To achieve the highest possible sensitivity, SOFAST-HMQC experiments are preferably performed on high-field NMR spectrometers equipped with cryogenically cooled probes. The duty cycle of over 80% in fast-pulsing SOFAST-HMQC experiments, however, may cause problems when using a cryogenic probe. Here we introduce SE-IPAP-SOFAST-HMQC, a new pulse sequence that provides comparable sensitivity to standard SOFAST-HMQC, while avoiding heteronuclear decoupling during ^1H detection, and thus significantly reducing the radiofrequency load of the probe during the experiment. The experiment is also attractive for fast and sensitive measurement of heteronuclear one-bond spin coupling constants.

© 2007 Elsevier Inc. All rights reserved.

Keywords: Duty cycle; Ernst angle; Fast data acquisition; Longitudinal relaxation enhancement; Selective pulses; Sensitivity enhancement; Proteins

Fast-pulsing NMR experiments provide a means for speeding up multi-dimensional NMR data acquisition. An example of fast-pulsing NMR is the SOFAST-HMQC experiment introduced recently [1,2] for recording two-dimensional heteronuclear ^1H – ^{15}N correlation spectra of proteins in only a few seconds. Short scan times of less than 100 ms are achieved by reducing the recycle delay between scans to almost zero. High sensitivity in this fast-pulsing regime is retained by Ernst-angle excitation [3] and longitudinal relaxation enhancement [4]. All ^1H pulses in SOFAST-HMQC are applied band-selectively, leaving the ^1H spins outside the excitation band unperturbed. For slowly tumbling molecules ($\omega_{\text{H}}\tau_{\text{c}} \gg 1$) such as proteins, this situation yields efficient energy dissipation from the excited ^1H spins to the unperturbed ^1H spins via dipolar interactions (spin diffusion). In addition, if the excited spins

are amide ^1H , amide–water hydrogen exchange also accelerates the return to thermal equilibrium. As a result of these effects, longitudinal ^1H relaxation times are reduced from more than a second to typically a few hundred milliseconds [1,4,5]. Furthermore, a polychromatic shaped ^1H excitation pulse [6] provides the variable flip-angle capabilities required for Ernst-angle excitation that further enhances the sensitivity of SOFAST-HMQC for very short recycle delays. An example of average sensitivity as a function of scan time, obtained for ^1H – ^{15}N SOFAST-HMQC of the small globular protein ubiquitin, is shown in Fig. 1c and compared to the results obtained using a conventional HSQC-based pulse scheme.

In order to achieve the highest possible sensitivity, protein NMR experiments are preferably performed on high-field NMR spectrometers equipped with a cryogenically cooled probe. Such equipment also provides the intrinsic sensitivity required for recording heteronuclear correlation spectra of proteins at sub-millimolar concentrations in a few seconds acquisition time [7]. Generally, duty cycles of

* Corresponding author. Fax: +33 4 38 78 54 94.

E-mail address: bernhard.brutscher@ibs.fr (B. Brutscher).

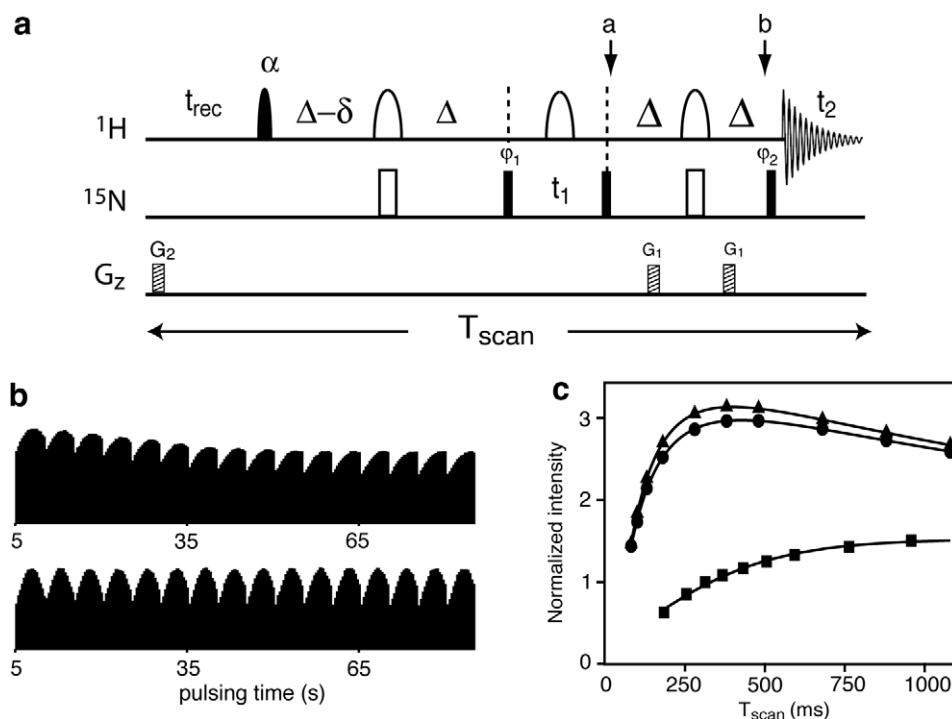


Fig. 1. (a) Pulse sequence for the sensitivity-enhanced (SE) IPAP-SOFAST-HMQC experiment. Filled and open pulse symbols indicate 90° and 180° rf pulses, except for the ^1H excitation pulse applied with flip angle α (with α chosen in the range $90^\circ < \alpha < 150^\circ$). The variable flip-angle ^1H pulse has a polychromatic PC9 shape [6], and band-selective ^1H refocusing is realized using REBURP [18]. The ^1H pulses are typically centered at 8.2 ppm and cover a band width of ~ 4.0 ppm, corresponding to pulse lengths of 2.25 ms (PC9) and 1.52 ms (REBURP) at 800 MHz. The transfer delay Δ is set to $1/(2J_{\text{HN}}) \approx 5.4$ ms, and the delay δ accounts for chemical shift and spin coupling evolution during about half of the PC9 pulse. Four repetitions of the experiment are recorded per t_1 increment with the following phase settings: (1) $\phi_1 = x$, $\phi_2 = y$, (2) $\phi_1 = x$, $\phi_2 = -y$, (3) $\phi_1 = y$, $\phi_2 = y$, (4) $\phi_1 = y$, $\phi_2 = -y$. The recorded time domain data sets are then combined as explained in the main text before Fourier transformation. The pulse sequence code for Varian spectrometers and processing protocols for NMR Pipe software are available from the authors upon request. (b) ^{15}N pulse width calibration curves recorded as a function of time for SOFAST-HMQC (upper panel) and SE-IPAP-SOFAST-HMQC (lower panel). The acquisition time was set to $t_2^{\text{max}} = 50$ ms, and low-power WURST-40 [19] decoupling ($\gamma B_1^{\text{rms}}/2\pi = 580$ Hz) was used for the standard version. The integrated spectral intensity is plotted as a function of time. The ^{15}N pulse width was first calibrated setting the recycle delay to $t_{\text{rec}} = 1$ s. Then a series of 15 1D spectra was recorded with the ^{15}N pulse width incremented from 80% to 120% of the initially determined optimal value, and setting the recycle delay to $t_{\text{rec}} = 1$ ms. This calibration series, taking about 5 s acquisition time each, was repeated for about 2 min (pulsing time) to monitor the effects of rf heating. (c) Average sensitivity of SOFAST-HMQC (triangles), SE-IPAP-SOFAST-HMQC (circles), and SE-HSQC (squares) as a function of scan time. The variable flip angle was set to $\alpha = 120^\circ$ for the two SOFAST-HMQC experiments. The sensitivity curves were obtained from integrating 2D spectral intensities measured for different recycle delays, normalized for equal experimental times.

a few percent are recommended when running NMR experiments on cryogenically cooled probes to maintain the probe temperature stable at about 25 K. Although it has been shown recently that fast-pulsing SOFAST-HMQC experiments with duty cycles on the order of 80% are not incompatible with cryogenic probes [8], the availability of a pulse sequence yielding similar minimal experimental times and comparable sensitivity to SOFAST-HMQC but with reduced radiofrequency (rf) load may still be of interest to reduce rf heating problems, and the risk of long-term damage of expensive cryogenic probes. The main source of rf heating in SOFAST-HMQC is the composite ^{15}N -decoupling applied during ^1H detection. Fig. 1b illustrates the kind of effects that may be observed when performing an ^{15}N -decoupled SOFAST-HMQC experiment with fast repetition rates ($T_{\text{scan}} < 100$ ms) on a high-field cryogenic probe: First, a slight detuning of the ^{15}N resonance circuit that increases the ^{15}N pulse width by up to 20%. Second, a drop in the detected NMR signal that can be ascribed to an

increased B_0 magnetic-field inhomogeneity. A stable situation is reached after about 1 min of pulsing. Interestingly, these effects are significantly less pronounced when ^{15}N -decoupling is avoided. In the absence of composite decoupling, steady-state conditions are reached after only a few seconds of pulsing. A way to avoid heteronuclear decoupling during ^1H detection is the use of an IPAP filter [9,10] where the 2 doublet components of a scalar (J)-coupled ^1H -X spin system are separated in different subspectra. A single correlation spectrum is obtained by adding the 2 subspectra after appropriate shifting of the 2 spectra along the ^1H dimension by an amount $\pm J/2$. This approach has first been proposed and applied to ^{13}C -detected NMR experiments in solids [11] and liquids [12] to remove homonuclear spin coupling-induced line splitting. The originally proposed IPAP version of SOFAST-HMQC, however, suffers from a $\sqrt{2}$ sensitivity loss with respect to the ^{15}N -decoupled experiment [2]. Here we introduce a sensitivity-enhanced (SE) version of IPAP-SOFAST-HMQC that

provides comparable sensitivity to standard SOFAST-HMQC, and therefore presents an attractive alternative in situations where the NMR experimentalist has to worry about radiofrequency load and duty cycle issues. It also allows the use of much longer t_2 acquisition times in situations where high resolution in the ^1H dimension is important. In addition, SE-IPAP-SOFAST-HMQC provides a tool for fast and sensitive measurement of (scalar and dipolar) ^1H - ^{15}N coupling constants, as demonstrated previously [2].

The pulse sequence of SE-IPAP-SOFAST-HMQC is shown in Fig. 1a. To simplify the following discussion we will focus on ^1H - ^{15}N correlation experiments, although the experiment is equally applicable to other heteronuclear ^1H -X two-spin systems, e.g. aromatic ^{13}C - ^1H and aliphatic $^{13}\text{C}^\alpha$ - $^1\text{H}^\alpha$ groups in proteins, or ^{13}C - ^1H groups in the sugar and base moieties of nucleic acids. In the standard SOFAST-HMQC sequence only one of the two ^{15}N quadrature components present after the t_1 evolution period is transferred into detectable ^1H coherence. This coherence transfer pathway, described by Eq. (1), is preserved in the SE-IPAP-SOFAST-HMQC sequence of Fig. 1a, while a second coherence transfer pathway, given by Eq. (2), also contributes to the detected NMR signal. Chemical shift evolution of the multiple-quantum coherence $2\text{H}_y\text{N}_x$ present at time point 'a' is refocused by a pair of ^1H and ^{15}N 180° pulses. Then an antiphase coherence $2\text{H}_y\text{N}_z$ is created at time point 'b' by an additional ^{15}N 90° pulse.

$$\text{Pathway(I)} : \dots \xrightarrow{t_1} 2\text{H}_y\text{N}_y \cos(\omega_{\text{N}}t_1) \xrightarrow{90^\circ\text{N}} 2\text{H}_y\text{N}_z \cos(\omega_{\text{N}}t_1) \\ \xrightarrow{2A} \text{H}_x \cos(\omega_{\text{N}}t_1) \xrightarrow{90^\circ\text{N}} \text{H}_x \cos(\omega_{\text{N}}t_1) \quad (1)$$

$$\text{Pathway(II)} : \dots \xrightarrow{t_1} 2\text{H}_y\text{N}_x \sin(\omega_{\text{N}}t_1) \xrightarrow{90^\circ\text{N}} 2\text{H}_y\text{N}_x \sin(\omega_{\text{N}}t_1) \\ \xrightarrow{2A} 2\text{H}_y\text{N}_x \sin(\omega_{\text{N}}t_1) \xrightarrow{\pm 90^\circ\text{N}} \pm 2\text{H}_y\text{N}_z \sin(\omega_{\text{N}}t_1) \quad (2)$$

In the absence of ^{15}N -decoupling the 2 coherence transfer pathways are detected as inphase (I) and antiphase (II) J_{NH} -doublets during ^1H detection. Contrary to the usual planar-mixing-based sensitivity-enhanced quadrature detection scheme [13], the detection of the 2 orthogonal pathways is achieved without additional transfer delays. The 2 pathways can be separated experimentally by adding (I) and subtracting (II) a second data set recorded with a 180° phase shift of the last 90° ^{15}N pulse (φ_2) yielding NMR signals with the following time modulation functions:

$$R_{\text{IP}} : \cos(\omega_{\text{N}}t_1) \cos(\pi J t_2) \exp(i\omega_{\text{H}}t_2) \quad (3)$$

$$R_{\text{AP}} : \sin(\omega_{\text{N}}t_1) \sin(\pi J t_2) \exp(i(\omega_{\text{H}}t_2 + \pi/2)) \quad (4)$$

Additional 90° phase incrementation of φ_1 as usual for quadrature detection in the ^{15}N dimension yields the 2 additional components:

$$I_{\text{IP}} : \sin(\omega_{\text{N}}t_1) \cos(\pi J t_2) \exp(i\omega_{\text{H}}t_2) \quad (5)$$

$$R_{\text{AP}} : \cos(\omega_{\text{N}}t_1) \sin(\pi J t_2) \exp(i(\omega_{\text{H}}t_2 + \pi/2)) \quad (6)$$

After complex two-dimensional Fourier transformation (2D FT) of $R_{\text{IP}} + iI_{\text{IP}}$ and $R_{\text{AP}} + iI_{\text{AP}}$, and appropriate phasing, 2 spectra are obtained with inphase (IP) and antiphase (AP) J_{NH} -splitting along the ^1H dimension. Note that this sensitivity enhancement scheme is similar to sensitivity-enhanced HSQC-type pulse sequences previously proposed for the measurement of heteronuclear coupling constants [14,15], and for multiplet component selection in C^α - C' correlation experiments [16].

The signal-to-noise (S/N) ratio in each of these IP and AP spectra is a factor of 2 lower than in a conventional ^{15}N -decoupled SOFAST-HMQC spectrum recorded under identical conditions because of the observed line splittings in the ^1H dimension. Addition and subtraction of these IP and AP spectra separates the upfield and downfield components of the peak doublet into subspectra (Fig. 2a), and increases the S/N ratio by a factor $\sqrt{2}$. To further increase the signal-to-noise ratio by a factor $\sqrt{2}$, the two single-transition state spectra are shifted in frequency by $\Delta\nu = \pm J/2$ with respect to each other, and added (Fig. 2b). This is possible because the scalar one-bond J -couplings differ only little from one nuclear site to the other. Overall, if spin-relaxation and pulse-imperfection-induced signal loss can be neglected, the SE-IPAP and standard SOFAST-HMQC experiments are expected to yield the same overall sensitivity for backbone amide groups. For the NH_2 groups of Asn and Gln side chains, the multiple-quantum coherence $2\text{H}_y\text{N}_x$ present between time points 'a' and 'b' in the sequence of Fig. 1a is transformed by the scalar coupling with the additional ^1H spin into $4\text{H}_y\text{N}_y\text{H}_z$ that is not converted into detectable ^1H coherence by the final ^{15}N 90° pulse. Therefore only pathway (I) is detected for NH_2 groups, and each of the two NH_2 correlation peaks appears as a 1:2:1 triplet motif along the ^1H dimension in the final SE-IPAP-SOFAST-HMQC spectrum (Fig. 2c). The single-transition state spectra shown in Fig. 2a also allow the measurement of the heteronuclear spin coupling constants from the relative peak position in the ^1H dimension. This may be of interest for the fast measurement of ^1H - ^{15}N residual dipolar couplings (RDCs) during the course of a kinetic reaction such as protein folding that can be monitored by real-time 2D NMR spectroscopy [7]. Such kinetic RDC measurements will provide valuable information about structural changes occurring during the kinetic event.

We have experimentally compared the sensitivity obtained for the new SE-IPAP-SOFAST-HMQC and the conventional SOFAST-HMQC pulse schemes. The experiments were performed on a Varian Inova 800 spectrometer equipped with a coldprobe using a 1.9 mM sample of ^{15}N -labeled ubiquitin at 25°C . Despite the increased number of ^{15}N rf pulses required for SE-IPAP-SOFAST-HMQC, a comparable overall sensitivity is observed for very short recycle delays using the same

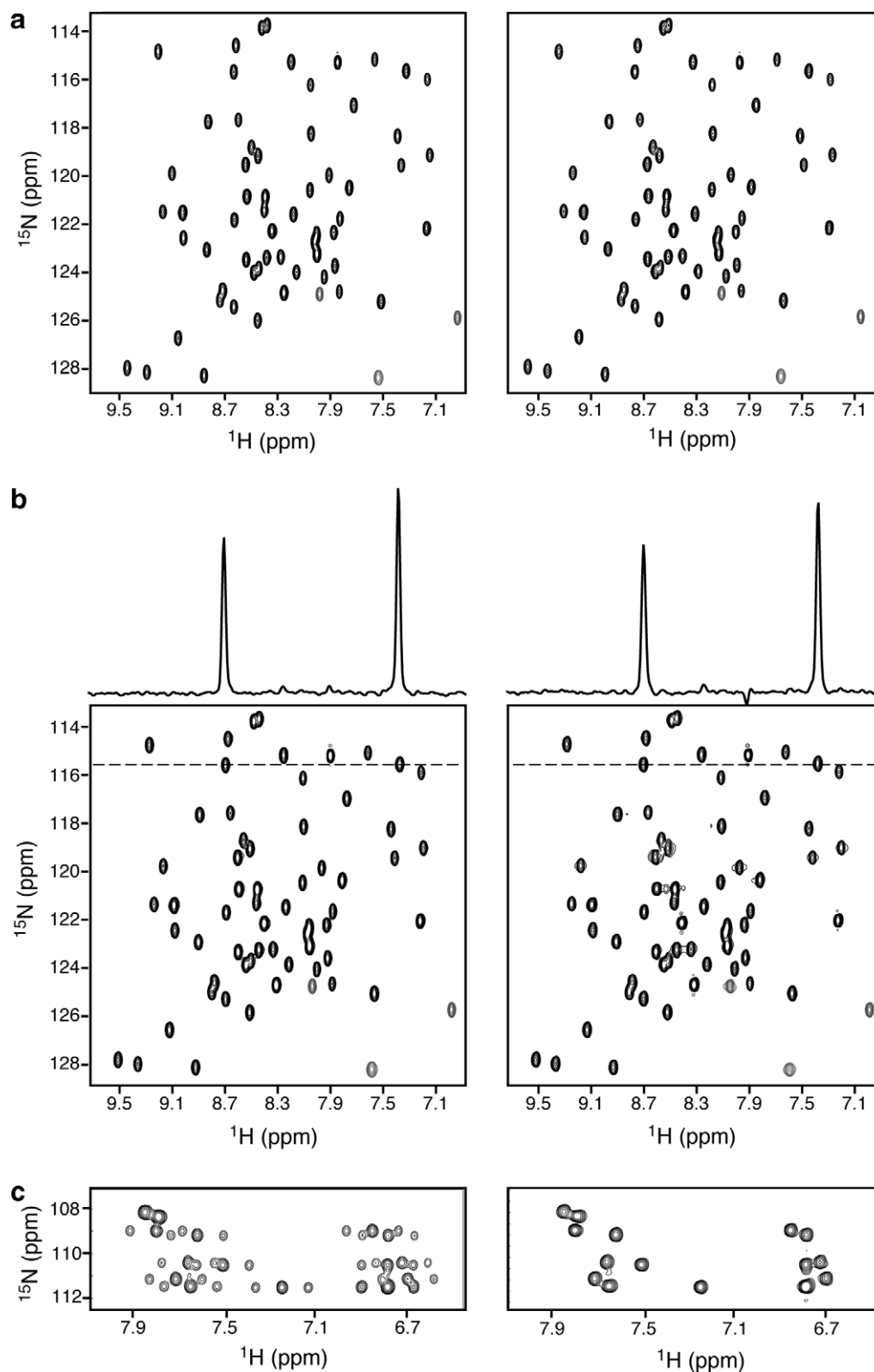


Fig. 2. ^1H - ^{15}N SE-IPAP-SOFAST-HMQC spectra (central region) of ubiquitin (1.9 mM, pH 6.3) recorded at 25 °C on a 800 MHz Varian spectrometer equipped with a coldprobe. The acquisition times were set to $t_1^{\text{max}} = 28$ ms and $t_2^{\text{max}} = 50$ ms, and the recycle delay to $t_{\text{rec}} = 1$ ms, resulting in an experimental time of 30 s. The spectra shown correspond to the result of different processing steps as explained in the text. (a) Single-transition state spectra, where the 2 doublet components are detected in different subspectra. These spectra are useful for the measurement of ^1H - ^{15}N coupling constants. (b) Final SE-IPAP-SOFAST-HMQC spectrum (left) obtained by adding the spectra shown in (a) after shifting them by ± 46.5 Hz with respect to each other along the ^1H dimension. A standard SOFAST-HMQC spectrum, recorded on the same ubiquitin sample in the same overall experimental time using identical acquisition parameters, is shown in the right panel for comparison. Additional 1D ^1H traces, extracted at a ^{15}N frequency of 115.6 ppm, are plotted for a better appreciation of the S/N ratios. (c) NH_2 region of the SE-IPAP-SOFAST-HMQC (left) and SOFAST-HMQC (right) spectra.

number of scans (see Figs. 1c and 2b). For longer recycle delays the standard pulse sequence performs slightly better (Fig. 1c) mainly because of the smaller number of rf pulses. The maxima of the sensitivity curves shown in Fig. 1c are reached at similar scan times (T_{scan}) indicating that the aliphatic and water ^1H polarization are only little affected by the additional ^1H pulses in the SE-IPAP-SOFAST-HMQC experiment. The minimal experimental time required for SE-IPAP-SOFAST-HMQC, however, is twice as long as for standard SOFAST-HMQC because a total of 4 (instead of 2) repetitions of the basic pulse sequence need to be performed to obtain the different quadrature components (Eqs. (3)–(6)). Therefore in the same experimental time as required for SE-IPAP-SOFAST-HMQC, it is possible to record a standard SOFAST-HMQC using a two-times longer scan time (T_{scan}). In the fast-pulsing regime ($T_{\text{scan}} < 100$ ms) this will yield a sensitivity advantage for the standard SOFAST-HMQC version that should be preferred whenever radiofrequency heating is not a problem.

If one has to worry about radiofrequency heating, the SE-IPAP-SOFAST-HMQC pulse sequence provides a sensitive alternative for recording high-quality ^1H - ^{15}N “fingerprint” spectra of small proteins at sub-millimolar concentration in about 15 s data acquisition time on a high-field NMR spectrometer equipped with a cryogenic probe. This is demonstrated for a 0.4 mM sample of the 14 kDa protein α -lactalbumin in Fig. 3a. The absence of ^{15}N -decoupling in SE-IPAP-SOFAST-HMQC allows choosing longer acquisition times in the ^1H dimension without increasing the radiofrequency load of the probe. This is especially important when studying helical-rich proteins or partially unfolded systems characterized by reduced chemical shift dispersion in the amide ^1H spectrum. An example of a SE-IPAP-SOFAST-HMQC ^1H - ^{15}N correlation spectrum recorded in 15 s using an acquisition time $t_2^{\text{max}} = 70$ ms on a small highly dynamic α -helical protein is shown in Fig. 3b.

In conclusion, we have presented a new experiment, SE-IPAP-SOFAST-HMQC that provides comparable sensitivity to standard SOFAST-HMQC while avoiding ^{15}N composite decoupling during ^1H detection. Sensitivity enhancement is achieved by a slight modification of the originally proposed IPAP-SOFAST-HMQC pulse sequence that converts both orthogonal transverse ^{15}N components present after t_1 into detectable ^1H coherence. SE-IPAP-SOFAST-HMQC provides an attractive alternative to standard SOFAST-HMQC for recording ^1H - ^{15}N protein spectra in a few seconds, whenever, due to hardware limitations, the use of composite decoupling during detection is not recommended. It also allows the fast measurement of heteronuclear coupling constants. The sensitivity enhancement “trick” presented here is not limited to SOFAST-HMQC, but it is also applicable to many other IPAP-type NMR experiments. Examples are ^{13}C -detected correlation experiments recently proposed for *protonless* NMR of pro-

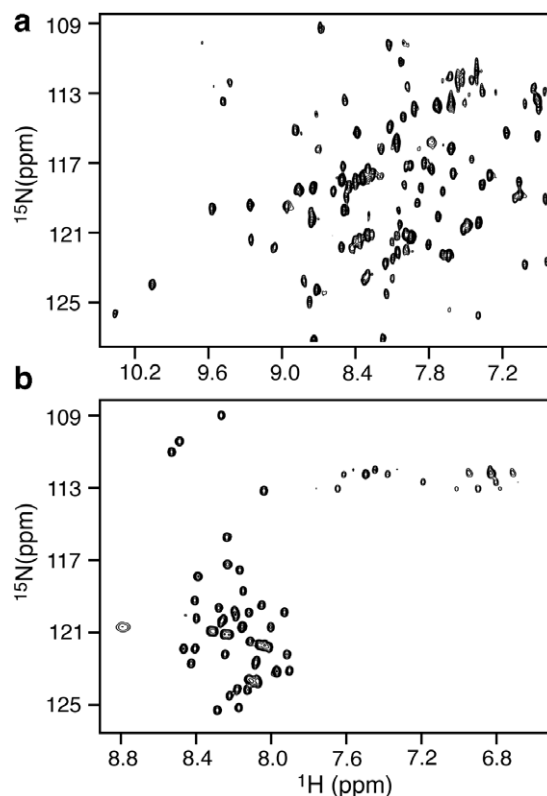


Fig. 3. SE-IPAP-SOFAST-HMQC spectra of 2 protein samples: (a) ^1H - ^{15}N spectrum of 0.4 mM α -lactalbumin (14 kDa). This spectrum, recorded in only 14 s, demonstrates the high sensitivity provided by the experimental setup. (b) ^1H - ^{15}N spectrum of a 63-residue highly dynamic α -helical protein. A long acquisition time $t_2^{\text{max}} = 70$ ms was chosen for optimal resolution in the detection dimension as most amide ^1H resonate within a spectral width of less than 1 ppm.

teins and nucleic acids [12,17] where line splitting due to homonuclear ^{13}C - ^{13}C couplings is removed by an IPAP filter.

Acknowledgments

This work was supported by the Commissariat à l’Energie Atomique, the Centre National de la Recherche Scientifique, the University Joseph Fourier (Grenoble), the French research agency (ANR-JCJC05-0077), and the European commission (EU NMR Contract No. 026145). T.K. and P.S. acknowledge support from the French ministry of education, research, and technology. The authors thank Dr. E. Lescop for stimulating discussions, and I. Ayala for the preparation of the labeled protein samples.

References

- [1] P. Schanda, B. Brutscher, Very fast two-dimensional NMR spectroscopy for real-time investigation of dynamic events in proteins on the time scale of seconds, *J. Am. Chem. Soc.* 127 (2005) 8014–8015.
- [2] P. Schanda, E. Kupce, B. Brutscher, SOFAST-HMQC experiments for recording two-dimensional heteronuclear correlation

- spectra of proteins within a few seconds, *J. Biomol. NMR* 33 (2005) 199–211.
- [3] R. Ernst, G. Bodenhausen, G. Wokaun, *Principles of Nuclear Magnetic Resonance in One and Two Dimensions*, Oxford University Press, Oxford, 1987.
- [4] K. Pervushin, B. Vögeli, A. Eletsky, Longitudinal H-1 relaxation optimization in TROSY NMR spectroscopy, *J. Am. Chem. Soc.* 124 (2002) 12898–12902.
- [5] M. Deschamps, I.D. Campbell, Cooling overall spin temperature: protein NMR experiments optimized for longitudinal relaxation effects, *J. Magn. Reson.* 178 (2006) 206–211.
- [6] E. Kupce, R. Freeman, Wide-band excitation with polychromatic pulses, *J. Magn. Reson. A* 108 (1994) 268–273.
- [7] P. Schanda, V. Forge, B. Brutscher, Protein folding and unfolding studied at atomic resolution by fast two-dimensional NMR spectroscopy, *Proc. Natl. Acad. Sci. USA* 104 (2007) 11257–11262.
- [8] J. Losoncz, E. Kupce, G. Gray, P. Sandor, B. Brutscher, Aligning ultrafast NMR spectroscopy and cold probe technology to reveal the mysteries of protein dynamics, *Am. Lab.* 38 (2006) 23–25.
- [9] M. Ottiger, F. Delaglio, A. Bax, Measurement of J and dipolar couplings from simplified two-dimensional NMR spectra, *J. Magn. Reson.* 131 (1998) 373–378.
- [10] P. Andersson, J. Weigelt, G. Otting, Spin-state selection filters for the measurement of heteronuclear one-bond coupling constants, *J. Biomol. NMR* 12 (1998) 435–441.
- [11] L. Duma, S. Hediger, B. Brutscher, A. Böckmann, L. Emsley, Resolution enhancement in multidimensional solid-state NMR spectroscopy of proteins using spin-state selection, *J. Am. Chem. Soc.* 125 (2003) 11816–11817.
- [12] W. Bermel, I. Bertini, I.C. Felli, M. Piccioli, R. Pierattelli, ¹³C-detected protonless NMR spectroscopy of proteins in solution, *Prog. Nucl. Magn. Reson. Spectrosc.* 48 (2006) 25–45.
- [13] A.G. Palmer, J. Cavanagh, P.E. Wright, M. Rance, Sensitivity improvement in proton-detected 2-dimensional heteronuclear correlation NMR-spectroscopy, *J. Magn. Reson.* 93 (1991) 151–170.
- [14] M.H. Lerche, A. Meissner, F.M. Poulsen, O.W. Sorensen, Pulse sequences for measurement of one-bond N-15-H-1 coupling constants in the protein backbone, *J. Magn. Reson.* 140 (1999) 259–263.
- [15] K.Y. Ding, A.M. Gronenborn, Sensitivity-enhanced E.COSY-type HSQC experiments for accurate measurements of one-bond ¹⁵N-¹H^N and ¹⁵N-¹³C' and two-bond ¹³C'-¹H^N residual dipolar couplings in proteins, *J. Magn. Reson.* 158 (2002) 173–177.
- [16] D. Lee, B. Vögeli, K. Pervushin, Detection of C' C^α correlations in proteins using a new time- and sensitivity-optimal experiment, *J. Biomol. NMR* 31 (2005) 273–278.
- [17] R. Fiala, V. Sklenar, ¹³C-detected NMR experiments for measuring chemical shifts and coupling constants in nucleic acid bases, *J. Biomol. NMR* 39 (2007) 153–163.
- [18] H. Geen, R. Freeman, Band-selective radiofrequency pulses, *J. Magn. Reson.* 93 (1991) 93–141.
- [19] E. Kupce, R. Freeman, Optimized adiabatic pulses for wideband spin inversion, *J. Magn. Reson. A* 118 (1996) 299–303.